J. Synchrotron Rad. (1997). **4**, 21–27

Application of an Imaging Plate to the Large-Volume Press MAX80 at the Photon Factory

J. Chen,*† T. Kikegawa, O. Shimomura and H. Iwasaki‡

Photon Factory, National Laboratory for High Energy Physics, 1-1 Oho, Tsukuba 305, Japan. E-mail: chen@sbmp04.ess.sunysb.edu

(*Received 21 June 1996; accepted 18 October 1996*)

An imaging plate was applied to the large-volume press MAX80 for quantitative *in-situ* X-ray diffraction. A combination of the two-dimensional detector with the uniform pressure and temperature environments of MAX80 and the wide energy range of synchrotron radiation resulted in high-quality diffraction data. A modified cell assembly with a disc-type heater was used to minimize extrinsic diffraction peaks from the surrounding materials. To demonstrate the high-quality data obtained from the imaging-plate system, the crystal structure of the high-pressure and high-temperature polymorph of the highly absorbing element bismuth (Bi IV) was determined.

Keywords: imaging plates; large-volume presses; high-pressure diffraction; powder diffraction; bismuth polymorphs.

1. Introduction

High-pressure *in-situ* powder diffraction is no longer only used for observing phase transitions and determining lattice parameters. *In-situ* structure determination and refinement is a growing trend in the high-pressure diffraction community (Chen, Iwasaki, Kikegawa, Yaoita & Tsuji, 1994; Nelmes & McMahon, 1994; Hamaya, Okabe, Yamakata, Yagi & Shimomura, 1996; Kunz *et al.*, 1996). To obtain this crystallographic information, accurate diffraction-intensity data combined with existing *d*-space data are indispensable. The quality of high-pressure diffraction data is mainly affected by pressure and temperature environments, sample quality, the X-ray source and the detecting instrument. The large-volume press offers a quasi-hydrostatic pressure environment, a large diffracting sample, easy heating and low temperature gradients. Synchrotron radiation is currently the best X-ray source for high-pressure diffraction, and many remarkable high-pressure diffraction experiments have been performed using synchrotron radiation (see *e.g.* Shimomura, 1986; Häusermann, 1992; Häusermann & Hanfland, 1996). However, there is a need to improve the detecting system for large-volume high-pressure apparatus. In this paper we describe the application of a two-dimensional detector, an imaging plate, to the large-volume press MAX80, and use the accurate diffraction data from this system to determine the crystal structure of Bi IV.

At the Photon Factory we have established a dual-dispersive X-ray diffraction (DDXD) system with the large-volume press MAX80 for quantitative diffraction (Kikegawa, Chen, Kenichi & Shimomura, 1995). In the DDXD system a step-scanning angle-dispersive X-ray diffraction (ADXD) mode is combined with an energy-dispersive X-ray diffraction (EDXD) mode in order to obtain a quantitative diffraction pattern as well as to allow quick sample identification and pressure determination. Nevertheless, it takes typically 4 h to acquire a quantitative diffraction pattern in the ADXD mode. Moreover, crystal grains often grow significantly due to high pressure and temperature, which results in spotty Debye–Scherrer rings and less-reliable intensity measurements. On the other hand, since an imaging plate (IP) was initially applied to a diamond-anvil-cell (DAC) system at the Photon Factory (Shimomura *et al.*, 1992), it has shown great potential in obtaining quick and reliable diffraction patterns from high-pressure studies (Nelmes *et al.*, 1992; Hamaya *et al.*, 1993; Fujihisa *et al.*, 1996; Kunz *et al.*, 1996). Having the advantages of high resolution, wide dynamic range, high efficiency, good uniformity of response, high sensitivity to short wavelengths and digital recording of the intensity (Amemiya & Miyahara, 1988), the imaging plate has become a widely adopted detector for diamond-anvil-cell systems at other synchrotron radiation sources, such as SRS Daresbury, ESRF, CHESS, Hasylab and SSRL.

Unlike a diamond-anvil cell, the large-volume press has a more complicated high-pressure cell geometry. The sample is surrounded by a capsule and heater, and is embedded in a solid pressure medium. Under pressure, the sample position and pressure must be determined by taking diffraction patterns. Moreover, because a collimator is not used in a two-dimensional detector system, diffracted X-rays from the surrounding materials will interfere with the sample diffraction pattern. All of these factors hinder the application of the imaging plate to the large-volume press. At the high-energy synchrotron radiation beamline of the Photon Factory, we have made attempts to overcome them.

† Present address: Center for High Pressure Research, Department of Earth and Space Sciences, State University of New York at Stony Brook, Stony Brook, NY 11794-2100, USA.

‡ Present address: Department of Physics, Faculty of Science and Engineering, Ritsumeikan University, Kusatsu, Shiga 525, Japan.

2. The MAX80 imaging-plate system

2.1. *Experimental design*

The imaging-plate system was installed at the high-energy synchrotron radiation beamline NE5C of the TRISTAN accumulation ring at the Photon Factory. A detailed description of the high-pressure dedicated beamline is given in a previous publication (Kikegawa *et al.*, 1989). Fig. 1 shows the layout of the system.

Since the system must have the capability of collecting rapid diffraction images as well as quantitative measurement, it is equipped with two detectors, an imaging plate and a solid-state detector (SSD). The imaging plate records accurate diffraction data using monochromatic X-rays. The solid-state detector is used for real-time diffraction measurements to map the cell geometry and determine the sample pressure with polychromatic X-rays, and for calibrating the energy of monochromatic X-rays. The solid-state detector is mounted on a 2θ goniometer arm which can move from +35 to −35°. An imaging-plate holder is mounted on a θ–φ two-way adjustable stage. The adjustments are rotations along a vertical axis (φ) and a horizontal axis (θ), which are perpendicular to the incident X-ray direction. The stage is movable along the incident X-ray direction on a guide block to change the sample-to-imaging plate distance (400–700 mm), and can be easily taken off from the guide block to allow the goniometer arm to move down for EDXD measurements. The imaging plate is a FUJI ST-V X-ray-use imaging plate of area 200 × 250 mm. The pixel size is 0.1 × 0.1 mm. When the imaging plate is used to record the diffraction pattern, the goniometer arm is rotated up to +35° The direct beam hits the top of the imaging plate to allow the largest number of diffraction lines to be detected. There is a set of receiving slits and a collimator mounted in the front of the solid-state detector to eliminate diffraction from the materials surrounding the sample. A special-design double-crystal monochromator (Kikegawa *et al.*, 1995) is used to select monochromatic X-rays. Two Si(111) single crystals are arranged in the (n, $-n$) configuration. The two crystals are positioned independently so that the radiation can be switched easily between monochromatic and polychromatic X-rays by simply moving the first crystal.

The large-volume press MAX80 is a cubic-type multi-anvil apparatus (Shimomura *et al.*, 1985). In Fig. 1, four side anvils out of six in the horizontal plane are shown. Under pressure, X-rays can only pass through the gaps between the anvils, as shown in Fig. 2. Most of the diffracted X-rays are masked by the side anvils. The diffraction pattern recorded on the imaging plate is a set of arcs from the full Debye–Scherrer rings. Fig. 3 shows an example of a diffraction pattern.

2.2. *Calibration and alignment*

The relation of energy and channel number for the solid-state detector was calibrated using fluorescence lines from various elements. These lines were fitted to a linear equation relating their energy and channel number. The energy of the monochromatic X-rays was then determined by the solid-state detector with an uncertainty of 0.01 keV. Alignment of the imaging plate was made by a technique adopted in the diamond-anvil-cell station (Shimomura *et al.*, 1992). As the majority of the Debye–Scherrer rings are masked by the anvils, the alignment must be made before the sample is loaded in the press in order to obtain entire Debye–Scherrer rings. The inclination angle (ψ) and centre offset (ε) can be minimized to $\psi \leq 0.02°$ and $\varepsilon \leq 0.01$ pixel (Shimomura *et al.*, 1992). The imaging plate-to-sample distance, L, could not be measured directly. Two exposures were made and L was determined using the formula $L = rD/(R - r)$, where D is the distance between the two exposures, and R and r are the radii of a Debye–Scherrer ring on the two exposures, respectively.

2.3. *Sample assembly and extrinsic diffraction peaks*

As there was no slit between the imaging plate and the sample, the imaging plate recorded all the diffraction from materials which intercept the incident X-ray. To minimize the extrinsic diffraction from the materials other than the sample, a cell assembly with disc heaters was adopted

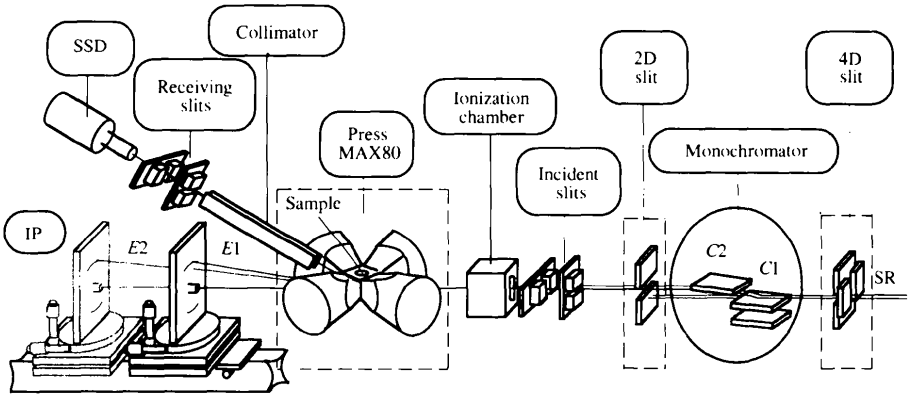

Figure 1
Layout of the imaging-plate diffraction system for the large-volume press MAX80 at the AR-NE5C beamline.

(Fig. 4*a*). The pressure medium was made of a mixture of four parts amorphous boron and one part epoxy resin.

The pressure medium has very little absorption; however, it gives several weak diffraction peaks at low angles in addition to the expected diffuse maxima from the amorphous material. The diffraction peaks were badly broadened so that they were very hard to fit during data processing. A sandwich-type pressure medium was therefore designed to avoid the extrinsic diffraction peaks (Fig. 4*b*). Two glass strips were embedded in the pressure medium to form a non-crystalline X-ray path. Consequently, the diffraction peaks from the boron–epoxy pressure medium were replaced by a smooth background. Fig. 5 shows a comparison of the diffraction patterns from boron nitride samples loaded in the ordinary disc-heater assembly (Fig. 5*a*) and in the sandwich-type assembly (Fig. 5*b*). The first two groups of diffraction peaks at low angles in Fig. 5(*a*), consisting of three and five peaks, respectively, are from the boron–epoxy pressure medium. They are totally removed in Fig. 5(*b*), and even at high angles the background of Fig. 5(*b*) becomes much smoother than that of Fig. 5(*a*). This improvement made the data analysis much easier.

Despite this benefit, glass is harder and more brittle than the pressure medium. Introducing glass strips into the pressure medium may upset the quasi-hydrostatic pressure environment and increase the possibility of blow-outs at high pressure. In case the sample diffraction peaks do not overlap with the boron–epoxy peaks, an ordinary disc-type assembly can be used, for which the data processing is not a problem. Furthermore, if the X-ray absorption coefficient of the sample is much greater than that of the pressure medium, the intensity ratio of the sample diffraction to the pressure-medium diffraction can be maximized by choosing the optimum X-ray energy. For example, the absorption of bismuth is greater than that of the pressure medium by a factor of two. Fig. 6 shows a series of diffraction patterns of bismuth collected using X-rays of different energy. The relative intensity of the sample diffraction to the pressure-medium diffraction increases when the X-ray energy increases from 40 to 60 keV. There is a best diffraction condition of $\mu t = 1$ (where μ is the linear absorption coefficient of the sample and t is the sample thickness). Because μ decreases with increasing energy and bismuth has a very large μ value ($\mu t > 1$), increasing X-ray energy makes μt of bismuth approach 1 while μt of the pressure medium ($\mu t < 1$) moves away from 1. The optimum energy was chosen by considering the best diffraction condition and the incident spectrum of the X-rays.

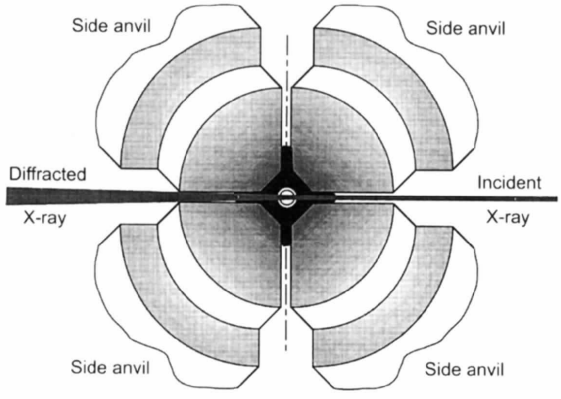

Figure 2
Top view of the geometry of the four side anvils in the horizontal plane and the X-ray path in MAX80.

2.4. *Experimental procedures*

To reach a desired pressure and temperature, the sample was first compressed stepwise in the press at room temperature. Diffraction patterns of an internal pressure marker (usually NaCl powder) and the sample were taken at each step, using the solid-state detector to determine the pressure by referring to Decker's scale (Decker, 1971) and to observe structure changes in the sample. When the desired pressure was reached or the diffraction pattern characteristic of a desired phase was observed, the sample was heated. A thermocouple was used to determine the sample temperature. Once the temperature reached a desired value or the diffraction pattern showed an expected characteristic, a diffraction pattern of the pressure marker was taken to check the pressure, and the location of the sample was mapped by diffraction with the solid-state detector. Then the radiation was switched to a monochromatic beam and

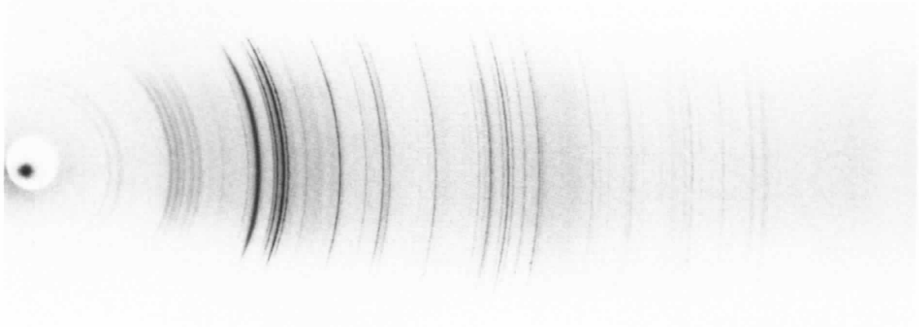

Figure 3
A diffraction pattern recorded on an imaging plate. Sample: Bi IV; X-ray energy: 49.67 keV; incident beam size: 0.2 × 0.5 mm; imaging plate-to-sample distance: 615 mm; exposure time: 30 min.

the press was moved to match the position of the incident beam. An imaging plate was mounted to the preset position while the goniometer arm was rotated up to +35°. The direct beam was exposed on the imaging plate for a second, then a beam stop was placed to stop the direct beam during the remaining exposure.

2.5. *Data processing*

The imaging-plate data were transferred off-line and digitized using a FUJI BAS2000 reader. The diffraction intensities were derived by integrating portions of the Debye–Scherrer rings recorded on the imaging plate. The program *IPH*, which was developed for the diamond-anvil cell–imaging plate system at the Photon Factory (Shimomura *et al.*, 1992), was used for the integration. Rietveld structure refinement (Rietveld, 1969) was processed by the program *PROFIL* (Cockcroft, 1990).

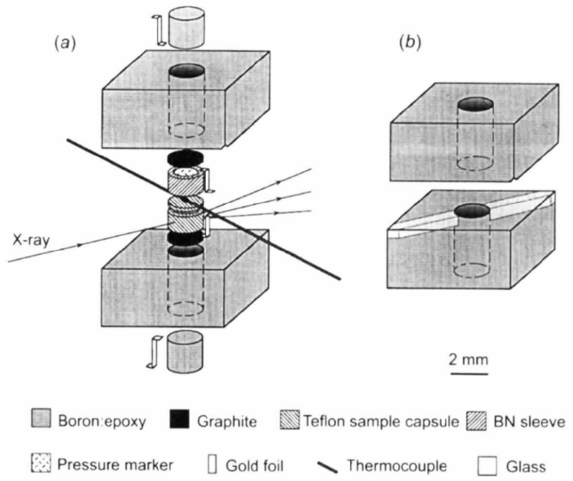

Figure 4
Assembly of the high-pressure cell with a disc-type heater. (*a*) A uniform pressure medium cube. (*b*) A sandwich-type pressure medium embedded with glass strips.

3. Crystal structure determination of Bi IV

Bismuth is known to undergo a number of polymorphic transitions under high pressure and temperature (Fig. 7; Cannon, 1974). Investigations have been made by previous researchers to determine the crystal structures of the high-pressure phases (Brugger, Bennion & Worlton, 1967; Brugger, Bennion, Worlton & Myers, 1969; Duggin, 1972; Schaufelberger, Merx & Contre, 1973; Fedotov, Ponyatovshii, Somenkov & Shil'shtein, 1979). Owing to complicated diffraction patterns and heavy absorption which make conventional X-ray diffraction difficult, there were no reliable structure data for Bi III, Bi III′ and Bi IV. We have successfully carried out structural studies on these phases with the diffraction system described above (Iwasaki, Chen & Kikegawa, 1995; Chen, Iwasaki & Kikegawa, 1996*a*,*b*). The remainder of this section discusses the structure determination of Bi IV.

Bi IV is a high-pressure and high-temperature phase which is stable in the pressure and temperature ranges 2.5–5.5 GPa and 450–550 K. The temperature range is narrow and close to the melting boundary. When the sample temperature was increased to the Bi IV stable range it was easy for the crystallite sample size to significantly increase, and therefore the quality of the diffraction pattern deteriorated. Using the imaging plate we could straightforwardly obtain information about the crystal size so we were able to optimize the *P*–*T* path for restraining the growth of crystal grains. A powdered sample was prepared at liquid-nitrogen temperature, and fine powders of an average size of 1 μm were collected by a flotation method. Details of the

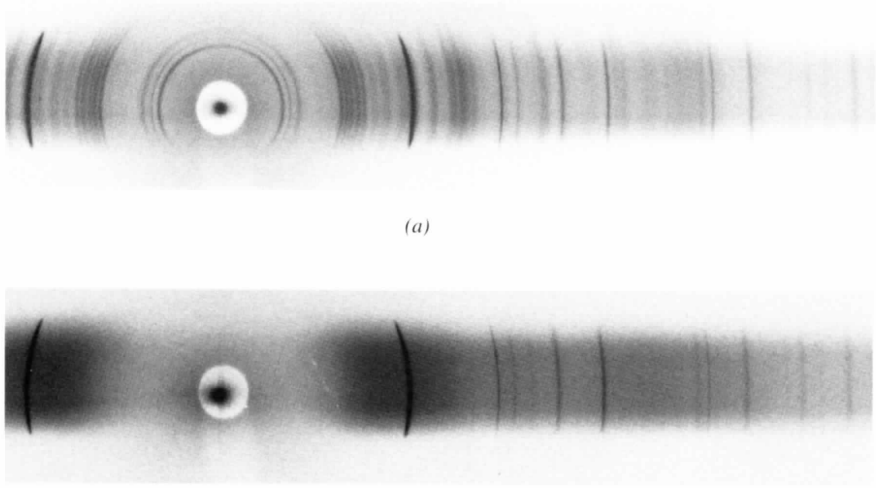

Figure 5
Comparison of imaging-plate diffraction patterns of boron nitride in (*a*) an ordinary pressure medium cube, and (*b*) a sandwich-type pressure medium cube embedded with glass strips. All the extrinsic peaks shown in (*a*) [compared with (*b*)] are from the boron–epoxy pressure medium.

sample preparation have been published elsewhere (Chen, Iwasaki & Kikegawa, 1996*a*). The sample was loaded together with a mixture of methanol and ethanol in a Teflon capsule to reach hydrostatic pressure conditions. As shown in Fig. 7, the sample was first heated close to the Bi IV–Bi V boundary at high pressure. The temperature was high enough for the sample to be free from the Bi III′ phase, and was far enough from the melting curve to avoid grain growth. The temperature and pressure were then changed from the Bi IV–Bi V boundary to the centre of the Bi IV stability field to eliminate the possible Bi V phase, and a diffraction pattern of Bi IV with good counting statistics was collected. Furthermore, integration along the Debye–Scherrer ring improved the powder averaging so that the diffraction data became more accurate.

The diffraction pattern for structure determination was taken at a pressure of 3.9 GPa and a temperature of 503 K, with an incident-beam cross section of 0.2 × 0.5 mm (Fig. 3). The optimized energy of the X-rays was 49.67 keV. Compared with the EDXD pattern and the step-scanning ADXD pattern, the resolution of the diffraction was greatly improved by using the imaging plate. Fig. 8 shows a comparison of the diffraction patterns taken by the three methods. Data analysis shows that Bi IV has a monoclinic crystal structure with space group $P2_1/c$, that eight atoms are contained in the unit cell, and that the lattice parameters are $a = 0.6468 \pm 0.0005$, $b = 0.6578 \pm 0.0005$, $c = 0.6468 \pm 0.0005$ nm, $\alpha = 118.88 \pm 0.06°$. Table 1 shows the atomic positions determined by Rietveld refinement (Fig. 9). The R factor $(\Sigma|I_{obs} - I_{cal}|/\Sigma I_{obs})$ is 0.16. The irregular profile of the background made it difficult to

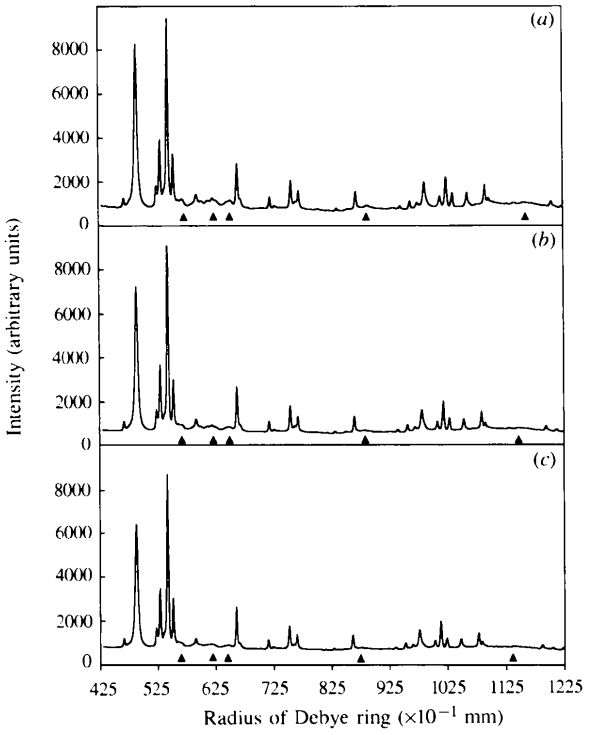

Figure 6
Comparison of diffraction patterns taken with different X-ray energies. (*a*) E = 40 keV, L (imaging plate-to-sample distance) = 483 mm. (*b*) E = 50 keV, L = 615 mm. (*c*) E = 60 keV, L = 726 mm. Solid triangles indicate diffraction peaks from the pressure medium.

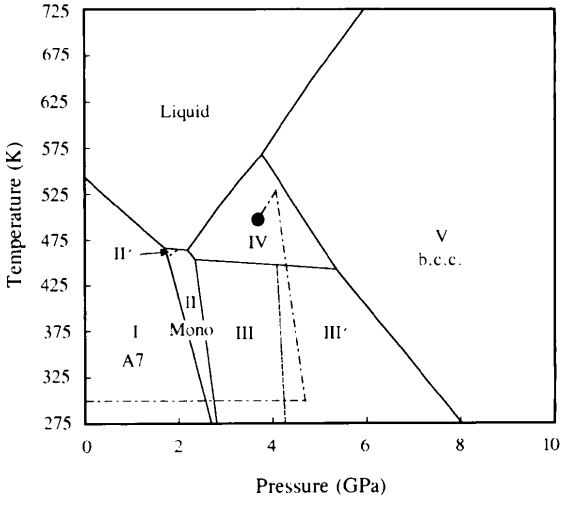

Figure 7
P–T phase diagram of bismuth (Cannon, 1974). Dashed lines show the optimum experimental *P–T* path for obtaining high-quality diffraction patterns of Bi IV.

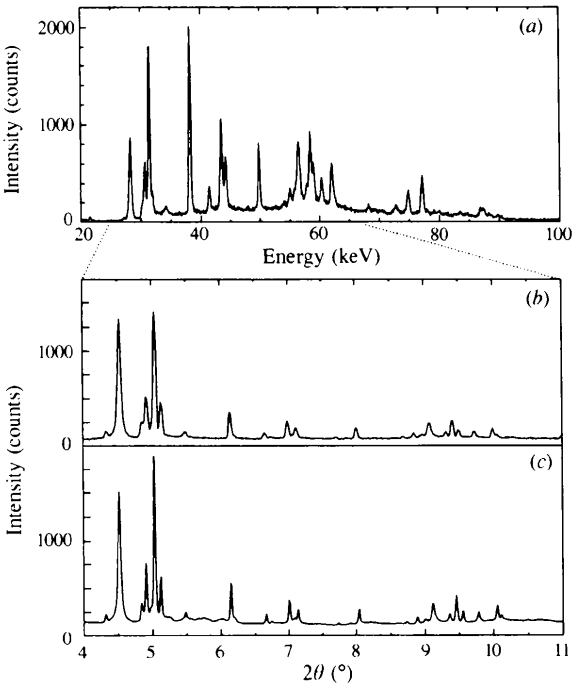

Figure 8
Comparison of diffraction patterns of Bi IV obtained by different diffraction methods. (*a*) Energy-dispersive diffraction with a solid-state detector. Fixed 2θ: 8°; recording time: 5 min. (*b*) Step-scanning angle dispersive diffraction with the solid-state detector. X-ray energy: 49.67 keV; scanning step: 0.01°; recording time: 240 min. (*c*) Two-dimensional recording angle dispersive diffraction with an imaging plate. X-ray energy: 49.67 keV; imaging plate-to-sample distance: 615 mm; exposure time: 30 min.

Table 1
Crystal structure parameters of Bi IV at 3.9 GPa and 503 K.

Position	x	y	z	B_{11}*	B_{22}	B_{33}	B_{13}
4(*e*)	0.3123 (7)	0.1775 (6)	0.3210 (7)	3.2 (5)	4.3 (7)	3.1 (5)	2.6 (5)
4(*e*)	0.2279 (6)	0.0039 (5)	0.1924 (6)	1.9 (2)	2.0 (2)	1.8 (2)	2.5 (2)

Space group $P2_1/c$. *Temperature factors are defined as: $\exp(-B_{11}X^2 - B_{22}Y^2 - B_{33}Z^2 - B_{13}\Phi)$, with $X = h/(2a\sin\beta)$, $Y = k/(2b)$, $Z = l/(2c\sin\beta)$ and $\Phi = hl\cos\beta/(2ac\sin^2\beta)$. Units of B are 10^{-2} nm^2.

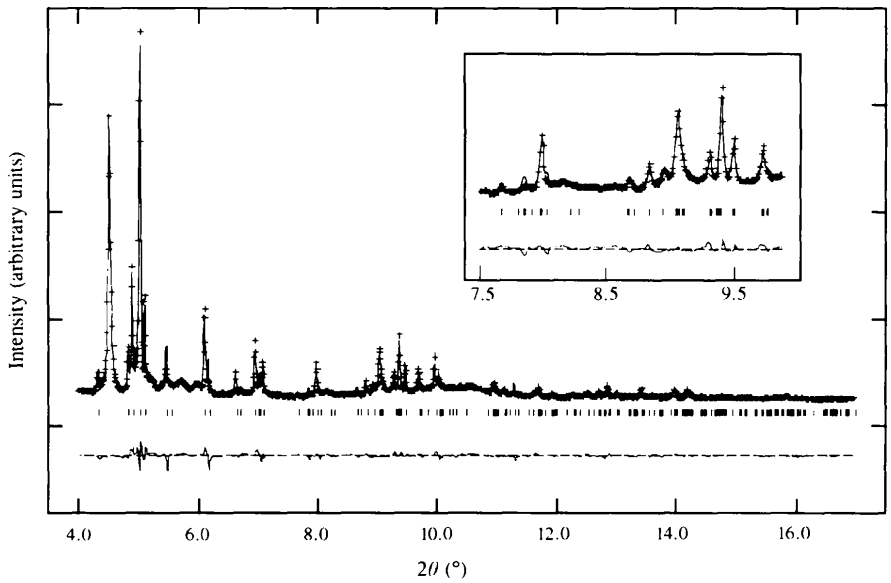

Figure 9
Rietveld fitting of the diffraction pattern of Bi IV at 3.9 GPa and 503 K. Crosses are observed data, the continuous line is the calculated profile, tick marks below the profile indicate the positions of allowed reflections, and the bottom curve shows the difference between the observed and calculated data. The inset shows a part of the enlarged profile.

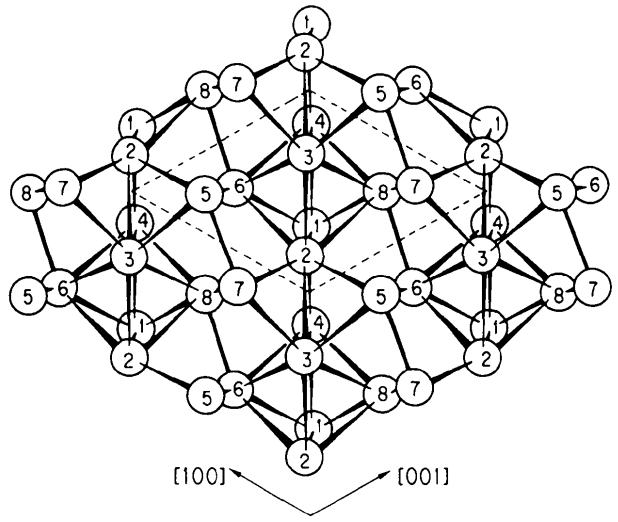

Figure 10
Structure of Bi IV. Broken lines represent the unit cell and bars between atoms show the nearest bonds.

reduce the value of the R factor further. A background-subtraction technique (Chen, Parise, Li, Weidner & Vaughan, 1996) may possibly improve the goodness-of-fit; however, the hydrostatic pressure condition will be worse when the liquid-holding capsule is removed. The crystal structure is shown in Fig. 10, which can be regarded as a distorted body-centred cubic structure (Chen, Iwasaki & Kikegawa, 1996*b*).

4. Conclusions

An imaging plate has been successfully applied to the large-volume press at the Photon Factory. The resolution of the diffraction pattern is improved by using the imaging plate. This makes the structure determination of non-quenchable, complex, high-pressure and high-temperature phases possible. Two-dimensional detection also gives information on the crystal size of the powdered sample under high pressure and temperature, allowing the assessment of the reliability of diffraction intensities. Integration gives a better powder averaging when crystal grains grow at high pressure and high temperature. These advantages allow us to perform accurate structure refinements for high-pressure and high-temperature phases. Combining the imaging-plate system and synchrotron radiation with a wide energy range enables us to obtain high-quality diffraction data for most samples. The two-dimensional diffraction technique is strongly recommended for applications to a large-volume press for quantitative diffraction measurements.

We would like to thank Professor Y. Amemiya at the Photon Factory for valuable discussions on the performance of the imaging plate. Thanks are also due to Dr P. J. Schields at State University of New York at Stony Brook for his critical reading of the manuscript. This work was performed under the approval of the Photon Factory Program Advisory Committee, proposal number 92G313.

References

Amemiya, Y. & Miyahara, J. (1988). *Nature (London)*, **336**, 89–90.

Brugger, R. M., Bennion, R. B. & Worlton, T. G. (1967). *Phys. Lett.* A**24**, 714–717.

Brugger, R. M., Bennion, R. B., Worlton, T. G. & Myers, W. R. (1969). *Trans. Am. Crystallogr. Assoc.* **5**, 141–154.

Cannon, J. F. (1974). *J. Phys. Chem. Ref. Data*, **3**, 781–824.

Chen, J., Iwasaki, H. & Kikegawa, T. (1996*a*). *J. Phys. Chem. Solids*. In the press.

Chen, J., Iwasaki, H. & Kikegawa, T. (1996*b*). *High Press. Res.* **15**, 143–158.

Chen, J., Iwasaki, H., Kikegawa, T., Yaoita, K. & Tsuji, K. (1994). *High-Pressure Science and Technology*, edited by S. C. Schmidt, J. W. Shaner, G. A. Samara & M. Ross, pp. 421–424. New York: AIP Press.

Chen, J., Parise, J. B., Li, R., Weidner, D. J. & Vaughan, M. T. (1996). Proc. USA-Jpn Meet. High Press. Geol. Sci. In the press.

Cockcroft, J. K. (1990). *PROFIL*. Version 4.03. ESRF, BP 220, F-38043 Grenoble CEDEX, France.

Decker, D. L. (1971). *J. Appl. Phys.* **42**, 3239–3244.

Duggin, M. J. (1972). *J. Phys. Chem. Solids*, **33**, 1267–1271.

Fedotov, V. K., Ponyatovshii, R. G., Somenkov, V. A. & Shil'shtein, S. Sh. (1979). *Sov. Phys. Solid State*, **20**, 628–632.

Fujihisa, H., Fujii, Y., Takemura, K., Shimomura, O., Nelmes, R. J. & McMahon, M. I. (1996). *High Press. Res.* **14**, 335–340.

Hamaya, N., Okabe, N., Yamakata, M., Yagi, T. & Shimomura, O. (1996). *High Press. Res.* **14**, 287–294.

Hamaya, N., Sakamoto, Y., Fujihisa, H., Fujii, Y., Takemura, K., Kikegawa, T. & Shimomura, O. (1993). *J. Phys. Condens. Matter*, **5**, L369–374.

Häusermann, D. (1992). *High Press. Res.* **8**, 723–737.

Häusermann, D. & Hanfland, M. (1996). *High Press. Res.* **14**, 223–234.

Iwasaki, H., Chen, J. & Kikegawa, T. (1995). *Rev. Sci. Instrum.* **66**(2), 1388–1390.

Kikegawa, T., Chen, J., Kenichi, Y. & Shimomura, O. (1995). *Rev. Sci. Instrum.* **66**(2), 1335–1337.

Kikegawa, T., Shimomura, O., Iwasaki, H., Sato, S., Mikuni, A., Iida, A. & Kamiya, N. (1989). *Rev. Sci. Instrum.* **60**, 1527–1530.

Kunz, M., Leinenweber, K., Parise, J. B., Wu, T. C., Bassett, W. A., Brister, K., Weidner, D. J., Vaughan, M. T. & Wang, Y. (1996). *High Press. Res.* **14**, 311–320.

Nelmes, R. J., Hatton, P. D., McMahon, M. I., Piltz, R. O., Crain, J., Cernik, R. J. & Bushnell-Wye, G. (1992). *Rev. Sci. Instrum.* **63**, 1039–1042.

Nelmes, R. J. & McMahon, M. I. (1994). *J. Synchrotron Rad.* **1**, 69–73.

Rietveld, H. M. (1969). *J. Appl. Cryst.* **2**, 65–71.

Schaufelberger, Ph., Merx, H. & Contre, M. (1973). *High. Temp. High Press.* **5**, 221–230.

Shimomura, O. (1986). *Physica*, **139/140B**, 292–300.

Shimomura, O., Takemura, K., Fujihisa, H., Fujii, Y., Ohishi, Y., Kikegawa, T., Amemiya, Y. & Matsushita, T. (1992). *Rev. Sci. Instrum.* **63**(1), 967–973.

Shimomura, O., Yamaoka, S., Yagi, T., Wakatsuki, M., Tsuji, K., Kawamura, H., Hamaya, N., Fukunaga, O., Aoki, K. & Akimoto, S. (1985). *Solid State Physics Under Pressure*, edited by S. Minomura, pp. 351–356. Tokyo: KTK Sci.